Why Do Grain Boundaries Exhibit Finite Facet Lengths?

J. C. Hamilton, Donald J. Siegel, Istvan Daruka,* and François Léonard
Sandia National Laboratories, Livermore, California 94551, USA
(Received 22 January 2003; published 20 June 2003)

Uniform finite facets are frequently observed at grain boundaries (GBs) and are usually attributed to equilibrium stabilization by GB stress. We report calculations for an aluminum twin GB using density functional theory, the embedded-atom method, and continuum elasticity theory. These methods show that GB stress is much too small to stabilize finite facets, suggesting that the usual explanation is incorrect.

DOI: 10.1103/PhysRevLett.90.246102 PACS numbers: 68.35.Ct, 61.72.–y, 68.35.Gy

High-energy grain boundaries (GBs) commonly undergo faceting to reduce their total energy. In many cases, the facets are observed to have uniform finite lengths, and the GB shows a sawtooth profile [1]. This self-organization of GB facets is important in determining mechanical properties of polycrystalline materials and in understanding the mechanisms of GB defaceting.

A particularly well-studied GB is the aluminum twin boundary with average $[1\bar{1}0]$ orientation, which separates two grains related to each other by a 180° rotation about a shared [111] axis. The faceting of this GB has been previously studied experimentally using transmission electron microscopy (TEM) [2]. At room temperature, this boundary spontaneously facets into regular $\Sigma 3\{11\bar{2}\}$-type facets with lengths of about 100 nm.

The equilibrium theory commonly invoked [1] to explain the finite facets is based on the premise that there exists a balance between attractive and repulsive forces between facet junctions. This is similar to the theory of stress domains on surfaces [3], where the energy cost of forming facet junctions is balanced by strain energy relief. As discussed below, for the GB, the repulsive force is due to the presence of dislocations at the facet junctions while the attractive force is due to GB stress. [We emphasize that GB stress is an interfacial stress (units of force/distance) not a bulk stress (units of force/area)].

There appear to be two reasons why a quantitative validation of the accepted theoretical explanation is still lacking. Experimentally, there are very few measurements of GB stress. (Recent x-ray diffraction measurements [4] have been used to estimate high-angle GB stress in Pd nanocrystals, but this is not a routine measurement). Theoretically, an explicit analytical expression for the energy of the faceted GB has not yet been presented, and atomistic calculations have not yet been performed to address this issue.

Here we combine continuum elasticity theory, density-functional theory (DFT), and embedded-atom method (EAM) calculations to show that the conventional energetic argument cannot possibly account for the experimental observations of finite facet lengths for the above aluminum GB with average $[1\bar{1}0]$ orientation. To do this, we first use continuum elasticity calculations to show that stabilization of finite facets arises when the GB stress exceeds a threshold value; for stresses below the threshold value, the energy is minimized by facets of infinite length. Using DFT and EAM, we show that the actual stress for the aluminum GB is much smaller than the threshold value, causing the equilibrium facet length to tend to infinity. Finally, this is confirmed by EAM calculations of the total energy as a function of facet length for the aluminum bicrystal with multiple GB facets.

We begin by discussing a planar GB to establish the key concepts of translation vector and GB stress. In general, GBs are characterized by a lower atomic density, which alters the equilibrium bond lengths compared to the bulk and induces a discontinuity in the spacing of lattice planes at the GB. The subset of lattice points forming a nearly continuous lattice across the GB is known as the coincident site lattice (CSL); the translation vector $\mathbf{t}$ measures the discontinuity in the CSL at the GB [5]. The lower atomic density at the GB also changes equilibrium bond lengths in the plane of the GB; however, this relaxation is only partial because of the coupling to the bulk lattice. Hence, the GB is in a state of stress [1], with a constant stress tensor component τ in the GB plane.

This description of the GB in terms of a translation vector and interfacial stress allows us to develop a simplified model of the faceted GB that is amenable to continuum elasticity calculations. Figure 1 shows a schematic of the faceted GB. When two GBs meet at an angle to form a facet junction, the translation vectors on the right, $\mathbf{t}_{\text{right}}$, and on the left, $\mathbf{t}_{\text{left}}$, are different, leading to a

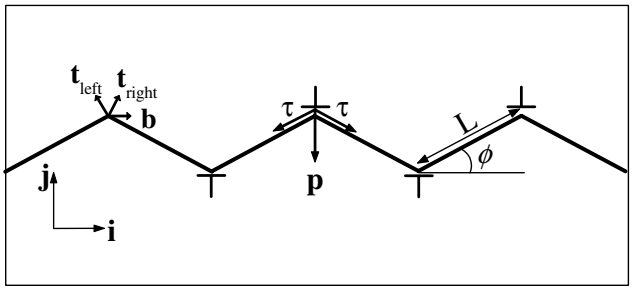

FIG. 1. Sketch of the GB used for the continuum elasticity calculations.

Burger's vector $\mathbf{b} = \mathbf{t}_{\text{right}} - \mathbf{t}_{\text{left}}$ at the facet junction [5]. At a junction between two facets, there is also a discontinuity of the stress tensor, leading to a line force $\mathbf{p}^n = \pm 2\tau \sin\phi\, \delta(x - x_n)\delta(y - y_n)\mathbf{j}$, where (x_n, y_n) is the position of the facet junction, ϕ is the GB angle, and the top (bottom) sign corresponds to a valley (crest). With this model of the faceted GB, we can now calculate its energy as a function of facet length L using isotropic continuum elasticity.

The energy of the GB per unit area can be written as

$$E = E_{d-d} + E_{lf-lf} + E_{d-lf}, \tag{1}$$

where E_{d-d} is the interaction energy between the dislocations, E_{lf-lf} is the interaction energy between the line forces, and E_{d-lf} is the interaction energy between the dislocations and the line forces (all of which include self-interactions). The three components of the energy can be calculated from

$$E_{\alpha-\beta} = -\frac{1}{2A}\sum_{m,n}\int f_i^{m\alpha}(\mathbf{r})u_i^{n\beta}(\mathbf{r}), \tag{2}$$

where $\alpha, \beta = d$ or lf, repeated indices imply summation, and A is the area of the unfaceted GB. Here, $f_i^{m\alpha}(\mathbf{r})$ and $u_i^{m\alpha}(\mathbf{r})$ are the force and elastic displacement caused by the mth dislocation or line force, in the $i = x, y$ or z direction. The displacements $u_i^{md}(\mathbf{r})$ are given in standard elasticity references [6] while $u_i^{mlf}(\mathbf{r})$ can be calculated from

$$u_i^{mlf}(\mathbf{r}) = \int G_{il}(\mathbf{r}-\mathbf{r}')p_l^m(\mathbf{r}'), \tag{3}$$

where $G_{il}(\mathbf{r})$ is the Green's function for an infinite isotropic elastic medium [6].

From the expressions above, we find that the energy is of the form $E(L) = (A/L)\ln L + B/L$ with

$$A = \frac{b^2\mu^2 - 2(3 - 4\sigma)(1 + \sigma)\tau^2\sin^2\phi + 4\tau b\mu\sin\phi(1 - 2\sigma)}{4\pi\mu(1 - \sigma)\cos\phi}, \tag{4}$$

and B is a constant that is unimportant for our purposes. Here σ is the Poisson ratio and μ is the shear modulus. From the functional form $E(L) = (A/L)\ln L + B/L$, one can show that finite facets will be stabilized when $A < 0$, leading to the condition

$$\tau > \frac{b\mu(1 - 2\sigma + \sqrt{7 - 6\sigma - 4\sigma^2})}{2(1 + \sigma)(3 - 4\sigma)\sin\phi} = \tau^*. \tag{5}$$

Hence, for finite facet lengths to be energetically favorable, the GB stress must exceed a threshold value τ^*.

Based on the above theory, the conventional explanation for the finite facet size observed at the Al twin boundary with average $[1\bar{1}0]$ orientation is that the GB stress τ is larger than τ^*. However, no experimental or theoretical values for τ or τ^* are available for this GB, making validation of the conventional model difficult.

In order to investigate this issue, we used DFT and EAM to calculate τ and τ^* for an Al $\Sigma 3$ $(1\bar{2}1)$ twin boundary. Our basic approach to obtain τ is to use a planar GB representing a facet and calculate the stress of this GB. To obtain τ^*, we calculate the translation vector $\mathbf{t}$ of this GB, obtain $\mathbf{b} = \mathbf{t}_{\text{right}} - \mathbf{t}_{\text{left}}$ and substitute in Eq. (5). We used a bulk slab with a small rectangular cross section and a long length in the $[1\bar{2}1]$ crystallographic direction. Periodic boundary conditions were used in all three directions. In order to ensure a completely stress-free bulk slab, the periodic lengths were relaxed in all three directions. Next, two equally spaced GBs were introduced with normals in the long $[1\bar{2}1]$ direction, as shown in Fig. 2. The slab periodic length, $L_{1\bar{2}1}$, in the direction normal to the GBs was then relaxed to allow for the excess volume of the GBs and the differing atomic density in the vicinity of the GBs. The translational vector $\mathbf{t}$ was calculated from the new periodic length in this long direction. Finally, we found the desired component of the GB stress by calculating the total system energy as a function of the appropriate periodic length, $L_{\bar{1}01}$, of the GB plane, while holding the other two periodic lengths fixed. A more complete description of these calculations follows.

Voter-Chen potentials for aluminum were used for the EAM calculations [7]. Our density-functional [8,9] calculations were performed with the *Vienna ab initio simulation package* (VASP) [10], which uses a plane-wave basis for expansion of the electronic wave functions combined with the generalized gradient approximation [11]

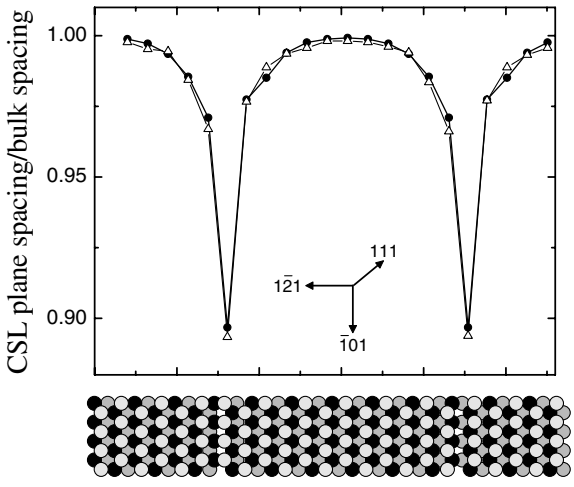

FIG. 2. Spacing of $(1\bar{2}1)$ CSL planes in Al with two $(1\bar{2}1)$ twin boundaries calculated from DFT (open triangles) and EAM (solid circles). Simulation supercell (replicated four times in the $[\bar{1}01]$ direction) is shown below the figure, with black circles representing atoms forming the CSL.

for the exchange-correlation energy. Ultrasoft pseudopotentials [12,13], including partial core corrections [14], were used to model the computationally expensive core-valence interaction. Brillouin zone sampling was performed using a Monkhorst-Pack grid [15], and electronic occupancies were determined according to a Methfessel-Paxton scheme [16] with an energy smearing of 0.15 eV. The number of k points was chosen to ensure that the elastic constants were converged to within 10% of the experimental values for bulk Al. This required the use of a very dense k grid ($40 \times 20 \times 2$), resulting in 400 irreducible k points. The plane-wave cutoff energy was set to 180 eV, which was sufficient to converge total energies to within 1–2 meV/atom.

For our DFT calculations, we started with a 72 atom GB-free bulk Al slab with periodic lengths $L_{\bar{1}01}$, L_{111}, and $L_{1\bar{2}1}$ in the three orthogonal slab directions. After careful relaxation of these periodic lengths to better than $\pm 0.1\%$ tolerance, we found $L_{\bar{1}01} = 2.864$ Å, $L_{111} = 7.005$ Å, and $L_{1\bar{2}1} = 59.376$ Å. In order to form two GBs, the central section of the unit cell was subjected to a reflection operation about a [111] mirror plane and two atoms were removed to create a 70-atom slab (shown relaxed and replicated in Fig. 2). The lengths $L_{\bar{1}01}$ and L_{111} were fixed at the bulk stress-free values and $L_{1\bar{2}1}$ was varied to minimize the total energy, thus allowing for the lower atomic density and the excess volume of the GB. Similar methods were used for the EAM calculations.

Figure 2 shows the spacing of the CSL planes in the presence of the GBs. Clearly, the CSL is contracted at the GBs compared to the bulk system; as explained above, the contraction occurs because the atomic density is lower at the GBs, leading to a decrease in the average coordination of each atom and slightly shorter bonds. As Fig. 2 clearly shows, we obtain excellent agreement between the DFT and EAM calculations, with a total contraction of the simulation cell in the $[1\bar{2}1]$ direction of 0.54 Å per GB for DFT and 0.51 Å for EAM [17]. Thus, taking the DFT result, the magnitude of the Burger's vector that enters in Eq. (5) is 0.54 Å. Our calculations are in good agreement with experiment [5] and previous calculations [5,18,19].

With this value for the Burger's vector and published values for the elastic constants of aluminum [20], we find from Eq. (5) that, for this particular GB, $\tau^* = 99$ meV/Å^2. The remaining question is whether the actual stress τ is above or below this value.

For the calculation of the GB stress, we used the slab from the previous calculation (shown in Fig. 2). L_{111} and $L_{1\bar{2}1}$ were fixed at their bulk stress-free values and the total energy was calculated as a function of $L_{\bar{1}01}$. The result of this calculation is plotted in Fig. 3, where the energy reference has been adjusted so the minimum of energy is at zero. As can be seen in the figure, the energy minimum is displaced from the bulk stress-free value because the GB stress has the effect of contracting the slab slightly in the $[\bar{1}01]$ direction. The GB stress is given by

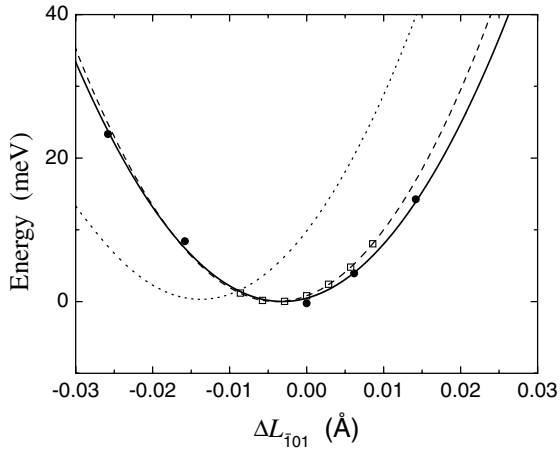

FIG. 3. Energy of the grain boundary of Fig. 2 as a function of the change in $L_{\bar{1}01}$ from its bulk stress-free value, calculated from DFT (solid circles) and EAM (open squares). The solid and dashed lines are quadratic fits. The dotted line is the energy calculated from Eqs. (7) and (8).

$$\tau = \frac{1}{2L_{111}} \frac{\partial E}{\partial L_{\bar{1}01}} \bigg|_{L_{\bar{1}01}=2.864\ \text{Å}}. \tag{6}$$

(The partial derivative is evaluated at the periodic length of the stress-free bulk slab). Using this method, we calculate a grain boundary stress of 21 meV/Å^2 using DFT and 29 meV/Å^2 using EAM. Given the uncertainties in the DFT and EAM calculations, these values agree within anticipated errors. The important point here is that both of these stresses are much smaller than the value $\tau^* = 99$ meV/Å^2 calculated above.

This large difference between the actual stress τ and the threshold stress τ^* can be further highlighted by comparing the DFT and EAM curves of Fig. 3 with a continuum elasticity calculation for a slab with two GBs having the threshold stress $\tau^* = 99$ meV/Å^2. Within continuum elasticity, the energy to deform the bulk slab (without the GB) is

$$E_{\text{bulk}} = \frac{V_0}{4}(C_{11} + C_{12} + 2C_{44})\left(\frac{\Delta L_{\bar{1}01}}{L_{\bar{1}01}}\right)^2, \tag{7}$$

where V_0 is the undeformed slab volume and the C_{ij} are the elastic constants. Adding the two GBs costs an additional energy,

$$E_{\text{GB}} = 2L_{111}\tau^* \Delta L_{\bar{1}01}. \tag{8}$$

The energy $E_{\text{bulk}} + E_{\text{GB}}$ is plotted as a dotted line in Fig. 3. Comparison of the DFT, EAM, and continuum elasticity curves shows agreement in the curvature, demonstrating that the atomistic calculations give the correct values for the bulk elastic constants. More importantly, the slope of the atomistic curves and the continuum elasticity curve are very different at $\Delta L_{\bar{1}01} = 0$. This reemphasizes that τ calculated from the atomistic calculations is much smaller than τ^*, demonstrating clearly that finite facets are not stabilized by GB stress at this grain boundary.

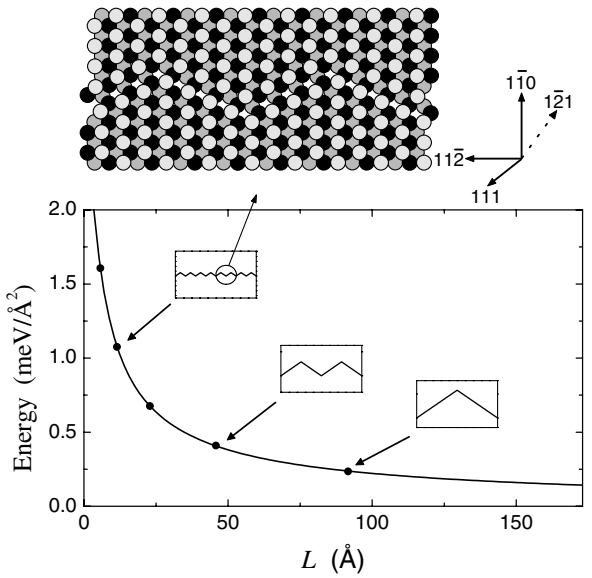

FIG. 4. Energy per unit area calculated by EAM for the Al GB with average $[1\bar{1}0]$ orientation faceted into $\Sigma 3$ $\{11\bar{2}\}$-type boundaries, as a function of facet length. The points are fit by the function $(A/L)\ln(L/1\text{ Å}) + B/L$. The insets show schematically the geometries used for some of the calculated points.

This conclusion can be directly verified by EAM calculations of the energy of a faceted Al boundary as a function of facet size using a geometry that replicates the experimental TEM observations. Figure 4 shows a schematic representation of a portion of this geometry. We modeled a 397 Å thick slab with two free $[1\bar{1}0]$ surfaces and a single GB with average $[1\bar{1}0]$ orientation in the center. The periodic boundary lengths in the [111] and $[11\bar{2}]$ directions were 7.01 and 158.7 Å, respectively. These boundary conditions were selected to allow modeling fairly long facets while avoiding interference of the GB strain field with the slab surface. For this bicrystal, we calculated the total relaxed energy with n facets of length 183.3 Å/n ($n = 2$, 4, 8, 16, and 32). All of these configurations contained the same number of atoms, the same area of free surface, and the same total GB area; thus, the changes in total energy directly reflect the GB energy as a function of facet length.

Figure 4 shows the calculated energy as a function of facet length L. The plotted points are well fit by a curve of the form $(A/L)\ln[L/(1\text{ Å})] + B/L$. Least squares fitting to the total EAM energies gives $A = 4.96$ meV/Å and $B = 1.54$ meV/Å. Since A is positive, there is no local minimum in the energy and no finite equilibrium facet length. The curve fit confirms what the plotted points suggest: The equilibrium GB facet length for the EAM calculation tends toward infinity, confirming the predictions from the continuum elasticity calculation.

As a final check of the above calculations and derivation, we can compare the values of A calculated from the EAM and the prediction from the elasticity calculation. From Eq. (4) and the values for b and τ from EAM, we find $A = 6.5$ meV/Å in good agreement with the EAM result $A = 4.96$ meV/Å. This is a strong check of the EAM calculations and of the continuum elasticity derivation.

The work presented here shows that finite facets are not equilibrium features of this GB. While the obvious alternative is kinetics, the actual atomistic kinetic mechanism remains to be explored, as does the generalization of the conclusion to other GBs.

We thank Norm Bartelt and Doug Medlin for useful discussions. This work was supported by the Office of Basic Energy Sciences, Division of Materials Sciences, U.S. Department of Energy under Contract No. DE-AC04-94AL85000. Part of I. D.'s work was supported by the OTKA Grant No. T037212.

*Present address: Department of Theoretical Physics, University of Debrecen, P.O. Box 5, H-4010, Debrecen, Hungary.

[1] A. P. Sutton and R. W. Balluffi, *Interfaces in Crystalline Materials* (Oxford University Press, New York, 1996).
[2] T. E. Hsieh and R. W. Balluffi, Acta Metall. **37**, 2133 (1989).
[3] V. I. Marchenko, Sov. Phys. JETP **54**, 605 (1981).
[4] R. Birringer, M. Hoffmann, and P. Zimmer, Phys. Rev. Lett. **88**, 206104 (2002).
[5] R. C. Pond and V. Vitek, Proc. R. Soc. London, Ser. A **357**, 453 (1977).
[6] L. D. Landau and E. M. Lifshitz, *Theory of Elasticity* (Butterworth-Heinemann, Stoneham, MA, 1995) 3rd ed.
[7] A. F. Voter and S. P. Chen, in *Characterization of Defects in Materials*, edited by R. W. Siegel, J. R. Weertman, and R. Sinclair (Materials Research Society, Pitttsburgh, PA, 1987), pp. 175–180.
[8] P. Hohenberg and W. Kohn, Phys. Rev. **136**, B864 (1964).
[9] W. Kohn and L. J. Sham, Phys. Rev. **140**, A1133 (1965).
[10] G. Kresse and J. Furthmüller, Phys. Rev. B **54**, 11 169 (1996).
[11] J. P. Perdew *et al.*, Phys. Rev. B **46**, 6671 (1992).
[12] D. Vanderbilt, Phys. Rev. B **41**, 7892 (1990).
[13] G. Kresse and J. Hafner, J. Phys. Condens. Matter **6**, 8245 (1994).
[14] S. G. Louie, S. Froyen, and M. L. Cohen, Phys. Rev. B **26**, 1738 (1982).
[15] H. J. Monkhorst and J. D. Pack, Phys. Rev. B **13**, 5188 (1976).
[16] M. Methfessel and A. T. Paxton, Phys. Rev. B **40**, 3616 (1989).
[17] There is also a CSL shift of 0.7 Å in the [111] direction at the GB. This shift cancels when subtracting the two facet translation vectors to get the Burger's vector for a GB facet junction.
[18] D. C. Medlin *et al.*, MRS Symp. Proc. **295**, 91 (1993).
[19] A. F. Wright and S. R. Atlas, Phys. Rev. B **50**, 15 248 (1994).
[20] J. P. Hirth and J. Lothe, *Theory of Dislocations* (Krieger, Malabar, FL, 1992), 2nd ed.